

Top-layer superstructures of the reconstructed Pt(100) surface

Klaus Kuhnke, Klaus Kern,* and George Comsa

*Institut für Grenzflächenforschung und Vakuumphysik des Forschungszentrums Jülich,
Postfach 1913, D-5170 Jülich 1, Federal Republic of Germany*

Wolfgang Moritz

*Institut für Kristallographie und Mineralogie der Ludwig-Maximilians-Universität München,
Theresienstrasse 41, D-8000 München 2, Federal Republic of Germany*

(Received 27 August 1991)

The structures of the two reconstructed phases of the Pt(100) surface have been studied by high-resolution helium diffraction. In contrast to earlier investigations, we show that for both phases the superstructure in the approximate $\langle 011 \rangle$ direction is not fivefold but much larger. The mean distance between atom rows in the top layer, however, is very close to that of a fivefold superstructure. This supports the description of the surface layer in a model which assumes static oscillations about a flat and equidistant atom arrangement. The results are discussed in comparison with low-energy electron diffraction, scanning-tunneling-microscopy, and x-ray-diffraction results.

Clean surfaces of transition metals display a fascinating variety of intrinsic reconstructions. Most of these are already well known from an experimental point of view and many theoretical efforts have been made to explain the structures found by experiment (see, e.g., Ref. 1). Within this variety, the surfaces of Pt(100), Ir(100), and Au(100) form a subclass. They display a quasi-hexagonal top layer on a square substrate lattice. Only Ir(100) is known to exhibit a comparatively small superstructure cell of (1×5) .^{2,3} Pt(100) and Au(100) reconstruct in unit cells of much larger size, where Pt(100) seemed to retain the fivefold superperiod of Ir(100) in one direction.⁴ It is generally assumed that the basic driving force for this type of reconstruction is the formation of a top layer with increased density. The details of the driving mechanism, however, are poorly understood and thus the reasons for the different behavior of the (100) faces of Pt, Ir, and Au are not clear.

We have applied helium diffraction for an investigation of the clean Pt(100) surface. This surface is of special interest since it can be prepared in two different phases, the metastable phase Pt(100)-hex and the stable phase Pt(100)-hex- $R0.7^\circ$.^{5,6} The measurements on both phases were performed at room temperature. Our analysis of the structural data provides information about the size of the unit cell. For both phases we have attempted a description with displacement waves which yields quantitative insight into the structure. Here we will only discuss the main results and refer the reader to a forthcoming paper for details.⁷

The Pt(100) sample was cleaned initially by heating for several hours at ≈ 900 K in an oxygen atmosphere of $\approx 10^{-8}$ mbar. Numerous cycles of sputtering with 1-keV argon ions followed by annealing were performed until the specular helium intensity was well reproducible.

Reaching this stage the width of the specular peak was limited by the instrumental resolution of 0.02 \AA^{-1} full width at half maximum at $E_{\text{He}} \approx 17.6$ meV. The reconstructed phases are largely unreactive and therefore rather insensitive to the residual gas. The base pressure in the sample chamber was 2×10^{-10} mbar and the surface was flashed to 1000 K before each experiment. The Pt(100)-hex metastable phase was prepared by sputtering followed by annealing for 5 min between 900 and 1000 K. The Pt(100)-hex- $R0.7^\circ$ phase was obtained after heating to 1300 K for several minutes. Both structures were checked with low-energy electron diffraction (LEED) and the typical patterns as known from the literature^{5,6,4} were observed. All helium diffraction measurements were performed with the total scattering angle fixed at 90° and a helium beam energy of 17.6 meV.

In our investigation we have found a splitting in the one-fifth-order peaks of the stable Pt(100)-hex- $R0.7^\circ$ phase which was so far assumed to display an exact fivefold superstructure. The polar diffraction scan along the row of split one-fifth-order peaks is presented in Fig. 1. The whole set of detected Bragg peaks is shown in Fig. 2(a). The peak positions were obtained from two-dimensional scans by successively changing the absolute value of parallel momentum transfer and rotating the sample around the surface normal.

The peak pattern in Fig. 2(a) can be separated into two sets of peaks. Each set stems from one rotational domain. Figure 2(b) displays the peaks ascribed to a single domain. The cross in Figs. 2(a) and 2(b) marks the position of the (10) peak obtained for the unreconstructed (1×1) phase. In this paper the indexing is with respect to the (1×1) surface structure. The diffraction pattern can be well approximated by a coincidence unit cell given in the matrix notation by $\begin{pmatrix} 13 & -1 \\ 18 & 43 \end{pmatrix}$. Using 2.77 \AA as the

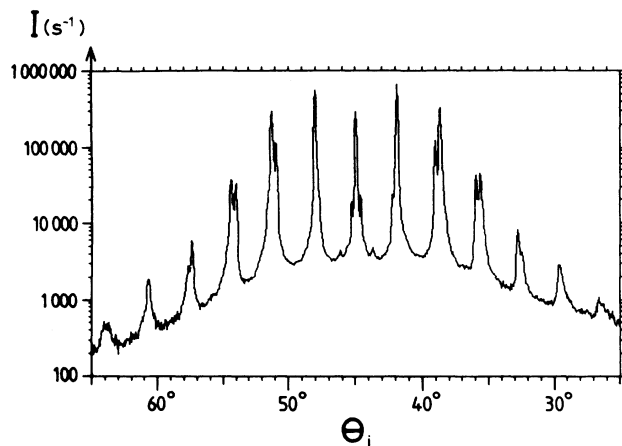


FIG. 1. Polar helium diffraction scan of the Pt(100)-hex-R0.7° phase 4.4° off the $\langle 011 \rangle$ direction. θ_i is the angle of incidence of the He beam at a fixed scattering geometry ($\theta_i + \theta_f = 90^\circ$) with $\lambda_{\text{He}} \approx 1.06 \text{ \AA}$; note the logarithmic intensity scale.

Pt(100)-(1 \times 1) lattice constant we obtain the reciprocal-lattice vectors: $\mathbf{b}_1^* \approx (0.1690, -0.0708) \text{ \AA}^{-1}$ and $\mathbf{b}_2^* \approx (0.0039, 0.0511) \text{ \AA}^{-1}$. In earlier LEED investigations the splitting of the one-fifth-order peaks could not be resolved and the coincidence cell was determined as $(1^4_1 \ 5^{-1})$. This description corresponds to a quasihexagonal top layer where the fivefold periodicity in the \mathbf{b}_2^* direction is preserved. Different authors obtained slightly different cells,^{6,4,3} probably due to different preparation conditions. The model for the real space structure assumed so far⁴ is based on domains of (1 \times 5) units similar to the quasihexagonal Ir(100)-(1 \times 5) unit cell. Stripes of different translational domains are considered to be separated by domain walls at a distance corresponding to approximately 14 substrate lattice constants. A regular arrangement of the parallel domain walls is assumed to explain the periodicity observed in a direction approximately perpendicular to the direction of the fivefold superstructure. The domain walls smooth out to a one-dimensional modulation of the atom rows. This corresponds to the picture of a quasihexagonal top layer in which the atom rows are slightly rotated against the

$\langle 011 \rangle$ symmetry direction of the crystal.

The line of intense peaks 4.4° off the $\langle 011 \rangle$ direction demonstrates [Figs. 1 and 2(b)] that the one-fifth-order peaks are split by $|\mathbf{b}_2^*| = 0.0512 \text{ \AA}^{-1}$. This observation leads us to an extension of the model because the fivefold superstructure cannot be exact. The supercells are longer than concluded from LEED investigations by a factor of 9. Still regarding the structure as a domain-wall system we have to postulate the occurrence of domain-wall crossings. The deviation from the fivefold periodicity was also found by a detailed comparison of top layer and substrate lattice vectors in a recent x-ray-diffraction study.⁸

We have analyzed the intensity ratio in the peak doublets as a function of the scattering vector (Fig. 1). As helium diffraction is only sensitive to the surface layer corrugation we reproduced the intensities by assuming a periodic vertical modulation of atomic positions. The agreement was best for nine oscillations per 53 top-layer rows. Thus we could identify the (10) peak of the quasihexagonal top layer with the 53 \mathbf{b}_2^* vector. The distance between the atom rows rotated by 0.7° against the $\langle 011 \rangle$ direction was therefrom calculated as 2.308 \AA ($\pm 0.004 \text{ \AA}$).⁷ This value corresponds to a contraction of $\approx 3.8\%$ compared to the hexagonal Pt(111) surface. The interrow distance in the $\langle 011 \rangle$ direction at room temperature can also be obtained from the x-ray scattering results by Gibbs *et al.*⁸ as 2.77 $\text{\AA}/1.204 = 2.301 \text{ \AA}$. The good agreement supports the validity of our corrugation model. For the length of one oscillation we obtain 13.6 \AA in agreement with the corrugation length observed by scanning-tunneling-microscopy.⁹

The second investigated structure is that of the Pt(100)-hex phase. Its Bragg peaks (Fig. 3) do not coincide with peaks of the Pt(100)-hex-R0.7° phase except for the peaks of integer order. As the pattern is well reproducible we will consider the Pt(100)-hex structure as a separate phase although it can also be regarded as an intermediate metastable state during the formation of the rotated phase. The peaks of the rotated phase begin to appear if the temperature during annealing is not kept well below 1100 K.

The structure factor again obtained from two-dimensional scans is shown in Fig. 3. It essentially con-

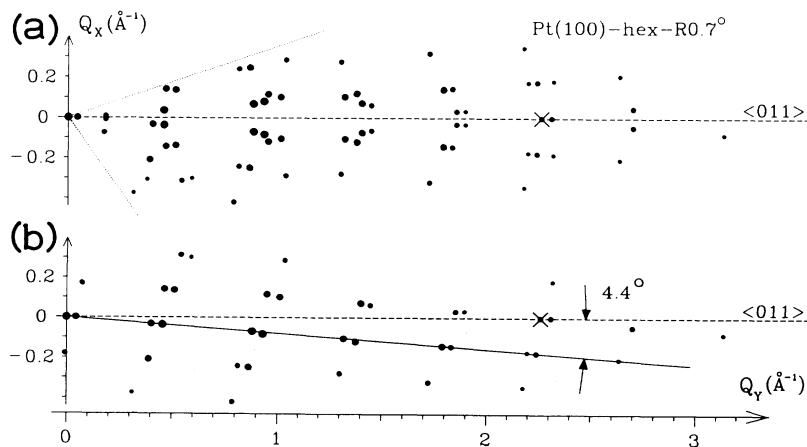


FIG. 2. (a) Structure factor of the Pt(100)-hex-R0.7° phase observed by helium diffraction ($E_{\text{He}} \approx 17.6 \text{ meV}$). The point diameter corresponds roughly to the logarithm of the peak intensities. They range from 600 000 to 200 counts per second per mA detector emission current. The pattern contains contributions from essentially two domains. The weak peaks at $Q_y \approx 0.2 \text{ \AA}^{-1}$ are due to another two domains rotated by 90°. The cross marks the (10) peak position of the unreconstructed Pt(100)-(1 \times 1) surface. Due to restrictions in the azimuthal rotation of the sample only the region between the dotted lines could be observed. (b) Contribution ascribed to a single domain.

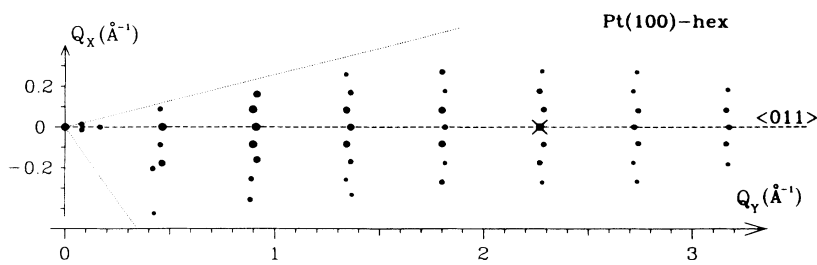


FIG. 3. Structure factor of the Pt(100)-hex phase ($E_{He} \approx 17.6$ meV). The contribution is mainly from one domain. The peaks close to the specular peak ($Q_y \leq 0.2 \text{ \AA}^{-1}$), however, are ascribed to the second domain, which is present due to the fourfold symmetry of the substrate lattice. All conventions are chosen as in Fig. 2. (The peak positions of three peaks at $Q_y \approx 0.4$ and 0.9 \AA^{-1} with large angular distances from the $\langle 011 \rangle$ direction display shifts from the expected positions which are probably due to instrumental deviations.)

tains peaks from one domain which obeys the $p2mm$ symmetry. At first sight the pattern resembles the $c(5 \times 25)$ pattern that was observed with LEED.^{5,4} The satellites of the one-fifth-order peaks, however, are not arranged on a straight line but display W shapes. This is unambiguously demonstrated by Fig. 4, which reproduces the intensity distribution close to the $\frac{3}{5}$ order position ($Q_y \approx 1.36 \text{ \AA}^{-1}$). After the transformation to Cartesian coordinates only two different values of Q_y are obtained for the eight peak maxima. The full pattern of Fig. 3 is described by $c(26 \times 150)$ in Wood's notation.¹⁰ It should be emphasized that the area of the unit cell is even larger than the one of the rotated phase by a factor of 6.

We may speculate that the metastable Pt(100)-hex supercell is composed of four parts that already resemble the stable phase with atom rows rotated 0.7° from the $\langle 011 \rangle$ direction. Especially the fact that the unit cell width for the rotated phase is 13 units compared to 26 units for the metastable phase supports a checkerboard

model in which black and white squares would correspond to regions of opposite rotational sense. This corresponds to a primary horizontal modulation of the atomic rows in the top layer.

On the $Q_x = 0$ line the superstructure peaks are found to correspond to exact one-fifth-order positions to better than 2%. Our results are therefore compatible with a modulation of the fivefold periodicity where the mean top-layer row distance in the $\langle 011 \rangle$ direction is equal to

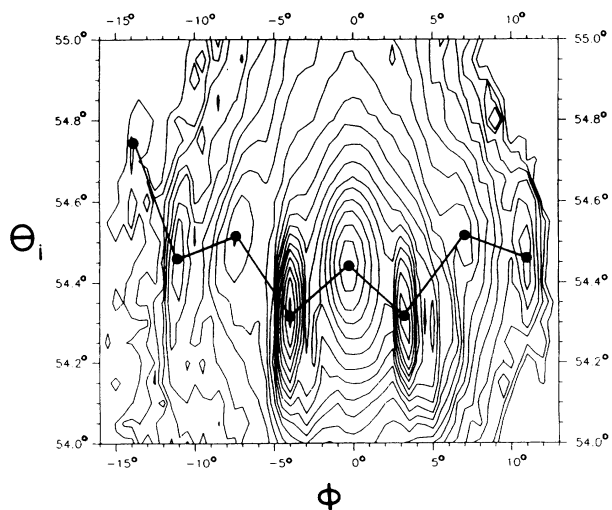


FIG. 4. Example of a two-dimensional scan at the $(\frac{3}{5} 0)$ position of Pt(100)-hex. The lines of equal intensity are drawn. In this presentation we have first subtracted a counting rate of 2200 s^{-1} from all measured points. Then the outermost line corresponds to a counting rate of 200 s^{-1} and proceeding from one line to the next corresponds to an increase in counting rate of 35%. θ_i is the angle of incidence of the He beam at a fixed scattering geometry ($\theta_i + \theta_f = 90^\circ$). ϕ is the azimuthal angle with $\phi = 0^\circ$ corresponding to the $\langle 011 \rangle$ direction; $\lambda_{He} \approx 1.06 \text{ \AA}$.

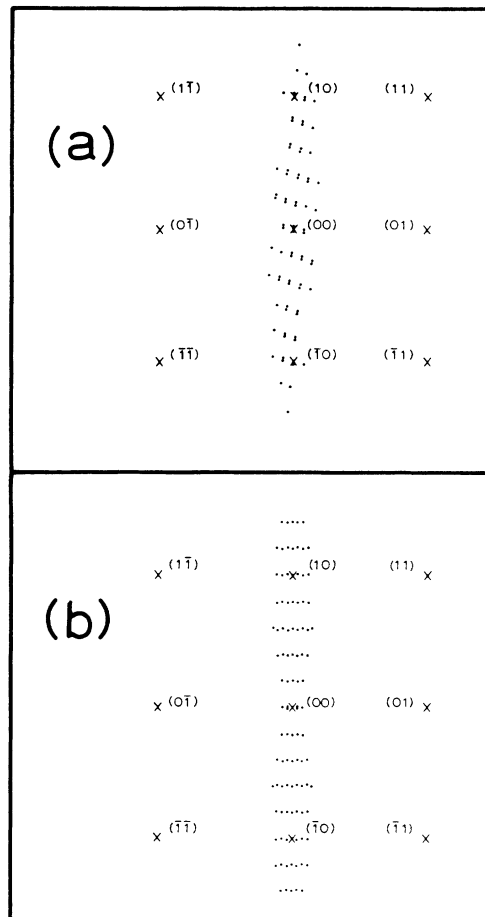


FIG. 5. Full diffraction patterns for a *single* domain of (a) Pt(100)-hex-R 0.7° and (b) Pt(100)-hex. These peak positions (full circles) are shown within the frame of the labeled peak positions of the unreconstructed surface (crosses). In (b) the three spurious peak positions mentioned in Fig. 3 have been omitted.

that of an exact (1×5) superstructure. The atomic arrangement must be different from that of the reconstructed phase on gold observed with LEED, namely Au(100)- $c(26 \times 68)$, in which characteristic deviations from the one-fifth-order positions were observed.^{4,2}

A comparison of the helium diffraction patterns for the two phases is shown in Fig. 5.

Helium diffraction is exclusively sensitive to the top-layer corrugation. Thus we can conclude that the large periodicity must already be present in the electron distribution at the surface. As helium diffraction is less sensitive to horizontal atomic displacements in a flat surface, the modulation is most likely caused by vertical displacements of the top layer, which will result from even small deviations from the fivefold periodicity.

The LEED patterns of both structures of Pt(100) closely resemble that of the helium diffraction experiment, with the difference being that the splitting and shifting of the peaks cannot be resolved. This indicates that multi-

ple scattering effects are less important for these large unit cells and that mainly the corrugation of the surface determines the LEED intensities of the satellite spots.

X-ray diffraction from the Pt(100)-hex- $R0.7^\circ$ surface has mainly observed peaks corresponding to top layer and bulk reciprocal-lattice vectors. In addition only harmonics of the hexagonal and substrate reflections were observed which may be due to the in-plane modulation of the top layer since multiple scattering effects should be negligible.

It becomes clear from this discussion that the features obtained with different methods contribute to a consistent picture in which the different observations can be explained in terms of the different capabilities of the methods.

This work was supported by the European Science Foundation.

*Present address: Institut de Physique Experimentale, Ecole Polytechnique Federale de Lausanne, PH-Ecublens, CH-1015 Lausanne, Switzerland.

¹K.-M. Ho and K. P. Bohnen, *Phys. Rev. Lett.* **59**, 1833 (1987), and references therein; F. Ercolessi, A. Bartolini, M. Garofalo, M. Parrinello, and E. Tosatti, *Surf. Sci.* **189/190**, 636 (1987); M. S. Daw, *ibid.* **166**, L161 (1986).

²E. Lang, K. Müller, K. Heinz, M. A. Van Hove, R. J. Koestner, and G. A. Somorjai, *Surf. Sci.* **127**, 347 (1983).

³W. Moritz, *Habilitationsschrift* (habilitation thesis), Ludwig-Maximilians-Universität, München, 1983.

⁴M. A. Van Hove, R. J. Koestner, P. C. Stair, J. P. Biberian, L.

L. Kesmodel, I. Bartos, and G. A. Somorjai, *Surf. Sci.* **103**, 189 (1981).

⁵J. J. McCarroll, *Surf. Sci.* **53**, 297 (1975).

⁶P. Heilmann, K. Heinz, and K. Müller, *Surf. Sci.* **83**, 487 (1979).

⁷K. Kuhnke, K. Kern, R. David, W. Moritz, and G. Comsa (unpublished).

⁸D. Gibbs, G. Grübel, D. M. Zehner, D. L. Abernathy, and S. G. J. Mochrie, *Phys. Rev. Lett.* **67**, 3117 (1991).

⁹R. J. Behm, W. Höslér, E. Ritter, and G. Binnig, *Phys. Rev. Lett.* **56**, 228 (1986).

¹⁰E. A. Wood, *J. Appl. Phys.* **35**, 1306 (1964).